Development 136, 1559-1570 (2009) doi:10.1242/dev.034066

Non-canonical Wnt signaling regulates cell polarity in female reproductive tract development via van gogh-like 2

Alysia L. vandenBerg and David A. Sassoon*

Wnt signaling effectors direct the development and adult remodeling of the female reproductive tract (FRT); however, the role of non-canonical Wnt signaling has not been explored in this tissue. The non-canonical Wnt signaling protein van gogh-like 2 is mutated in *loop-tail* (*Lp*) mutant mice (*Vangl2*^{Lp}), which display defects in multiple tissues. We find that *Vangl2*^{Lp} mutant uterine epithelium displays altered cell polarity, concommitant with changes in cytoskeletal actin and scribble (scribbled, Scrb1) localization. The postnatal mutant phenotype is an exacerbation of that seen at birth, exhibiting more smooth muscle and reduced stromal mesenchyme. These data suggest that early changes in cell polarity have lasting consequences for FRT development. Furthermore, Vangl2 is required to restrict Scrb1 protein to the basolateral epithelial membrane in the neonatal uterus, and an accumulation of fibrillar-like structures observed by electron microscopy in *Vangl2*^{Lp} mutant epithelium suggests that mislocalization of Scrb1 in mutants alters the composition of the apical face of the epithelium. Heterozygous and homozygous *Vangl2*^{Lp} mutant postnatal tissues exhibit similar phenotypes and polarity defects and display a 50% reduction in *Wnt7a* levels, suggesting that the *Vangl2*^{Lp} mutation acts dominantly in the FRT. These studies demonstrate that the establishment and maintenance of cell polarity through non-canonical Wnt signaling are required for FRT development.

KEY WORDS: Vangl2, Wnt, Female reproductive tract, Uterus

INTRODUCTION

Mammals possess male and female reproductive tract (FRT) anlage during early development (E13.5) (Yin and Ma, 2005). The Müllerian duct epithelium in mice remains undifferentiated until ~5 days after birth and consists of columnar epithelium surrounded by mesenchyme (Boutin et al., 1992; Cunha, 1976c; Glasser et al., 2002). Subsequently, the posterior epithelium stratifies in the presumptive cervix and vagina, while anterior epithelium forms the uterine horns and oviducts (Kitajewski and Sassoon, 2000; Yin and Ma, 2005). By 1 week of development, uterine epithelial glands and smooth muscle form, and by 2 weeks the FRT is differentiated. Epithelial-mesenchymal interactions underlie FRT development (Cunha et al., 2004; Cunha et al., 1992b; Kitajewski and Sassoon, 2000). In tissue recombination experiments, grafting perinatal Müllerian mesenchyme from presumptive vagina to epithelium from any part of the FRT induces stratified epithelium (Cunha, 1976b; Cunha et al., 1992b; Pavlova et al., 1994), demonstrating that the mesenchymal signals dictate epithelial fate. Mesenchyme grown alone develops entirely into smooth muscle (Boutin et al., 1992; Cunha et al., 1992a).

Wnt signaling molecules, including Wnt4 (Bernard and Harley, 2007; Miller et al., 1998b), Wnt5a (Mericskay et al., 2004; Miller et al., 1998b), Wnt7a (Carta and Sassoon, 2004; Miller et al., 1998a) and Wnt9b (Carroll et al., 2005), regulate FRT development. Wnt9b signals upstream of Wnt4 and both direct Müllerian tube formation (Carroll et al., 2005). At birth, *Wnt5a* mutants lack a cervix and vagina, and uterine horns are shortened and fused at the midline or terminate in a blind pouch (Mericskay et al., 2004). Neonatal *Wnt7a* mutants have a septate vagina, with small diameter uterine horns and a lack of oviduct coiling (Miller and Sassoon, 1998). Both *Wnt5a* (Mericskay et al., 2004) and *Wnt7a* (Miller et al., 1998a) mutant postnatal uterine tissues fail to form glands, and *Wnt7a* mutants display hyperplastic and disorganized smooth muscle with stratified uterine epithelium.

Wnt5a expression in the mesenchyme (Mericskay et al., 2004) and *Wnt7a* expression in the epithelium of the oviduct and uterus (Miller and Sassoon, 1998) are required for proper FRT development (Mericskay et al., 2004; Miller and Sassoon, 1998). In *Wnt7a* mutants, *Wnt5a* is expressed ectopically in epithelium and its expression declines by 12-16 weeks (Mericskay et al., 2004) and *Wnt4* expression is misregulated (Miller et al., 1998a). By contrast, *Wnt5a* mutants display a reduction in the expression of *Wnt4a*, whereas *Wnt7a* expression is unaffected unless challenged with estrogen (Mericskay et al., 2004).

Wnt molecules signal through three known pathways: the canonical β-catenin-dependent pathway (Logan and Nusse, 2004), non-canonical Ca^{2+}-mediated signaling (Wang and Malbon, 2003), and non-canonical signaling orchestrating cell migration and movement (Mlodzik, 2002). Transgenic mice lacking β-catenin in the mesenchyme of the FRT do not recapitulate the *Wnt5a* or *Wnt7a* mutant phenotypes (Arango et al., 2005; Deutscher and Hung-Chang Yao, 2007), suggesting that canonical Wnt signaling involves both pathways. We previously noted that *Wnt7a* knockout mice display changes in cell orientation of the FRT at birth (Miller et al., 1998a; Miller et al., 1998b). FRT developmental defects have been described for *loop-tail* mice that contain a point mutation in van gogh-like 2 (*Vangl2*^{Lp}) (Kibar et al., 2001), including a septate vagina (Murdoch et al., 2001; Strong and Hollander, 1949), cell polarity defects in the cochlea (Montcouquiol et al., 2003) and disruptions in cardiac outflow tract (Phillips et al., 2005) owing to defects in cell movement (Phillips et al., 2008).

Drosophila Strabismus (Van Gogh – FlyBase), the homolog of van gogh-like 2, is required for the planar cell polarity (PCP) establishment of eyes and wing bristles (Kibar et al., 2001; Wolff and Rubin, 1998). Core non-canonical Wnt signaling components, which are conserved in *Xenopus*, *Drosophila* and mammals,

Myology Group, UMR S 787 Inserm, Université Pierre et Marie Curie Paris VI, 105 bd de l'Hôpital, 75634 Paris Cedex 13, France.

*Author for correspondence (e-mail: david.a.sassoon@gmail.com)

Accepted 3 March 2009

coordinately regulate developmental processes requiring cell movement, including convergent extension, PCP in *Drosophila* eyes and wing bristles and in mouse cochlea, and murine epidermal hair patterning (Klein and Mlodzik, 2005). These signaling components have been investigated in *Xenopus* and *Drosophila*, and recent studies suggest a related function in mice. The proteins involved in neural tube closure include Wnt5a and Wnt11b (Hardy et al., 2008), frizzled 6 (Fzd6) (Guo et al., 2004; Wang et al., 2006b) and downstream non-canonical Wnt signaling components such as mouse Vangl2 (Montcouquiol et al., 2003; Phillips et al., 2005) and dishevelled 1 (Dvl1) and Dvl2 (Hamblet et al., 2002). PCP in mouse cochlea uses the same signaling module, as shown by defects observed in *Vangl2* mutants and in *Fzd3; Fzd6* and *Dvl1; Dvl2* double mutants (Montcouquiol et al., 2003; Wang et al., 2005; Wang et al., 2006b). PCP also functions in the murine epidermis: *Fzd6* mutants have whorled hair patterns (Guo et al., 2004) and *Vangl2* mutants display a loss of hair follicle polarization (Devenport and Fuchs, 2008).

Murine Vangl2 contains multiple PDZ domains, which mediate scribble (scribbled, Scrb1) binding (Montcouquiol et al., 2006b). Scrb1 also contains multiple PDZ domains and functions in cell polarity and migration in different capacities through interactions with multiple binding partners. In polarized epithelium, Scrb1 binds lethal giant larvae 2 (Lgl2) (Kallay et al., 2006) and functions with discs large (Dlg) to restrict the Par3-Par6 (Par) complex to the apical membrane (Macara, 2004). The Par complex, in turn, restricts the Scrb1 complex to the basolateral membrane (Bilder et al., 2003; Tanentzapf and Tepass, 2003). In *Drosophila*, loss of either Lgl, Dlg or Scribble induces expansion of the Par-expressing apical domain (Bilder et al., 2000), suggesting that these two groups of proteins reciprocally maintain the apical and basolateral domains. In mammalian MDCK cells, E-cadherin-mediated cell adhesion is disrupted by the loss of Scrb1 and restored by expression of an E-cadherin-catenin fusion protein (Qin et al., 2005), and Scrb1 interacts with the tight junction protein ZO-2 (Tjp2) as determined by immunoprecipitation (Metais et al., 2005), suggesting that it plays a role in cell-cell adhesion. In a process that is not well understood, Scrb1 is required to establish cell polarity for the migration of epithelial cells (Dow et al., 2007) and T-cells (Ludford-Menting et al., 2005), which might involve the ability of Scrb1 to bind p21-activated kinase (Pak) interacting exchange factor (β-PIX; Arhgef7) (Audebert et al., 2004), which activates GTPases such as Cdc42/Rac (Sinha and Yang, 2008). Other Vangl2 binding interactions in mice include the epithelial tight junction protein Magi3 (Laura et al., 2002; Yao et al., 2004) and Dvl1, Dvl2 and Dvl3 (Torban et al., 2004). The *Vangl2^{Lp}* mutation genetically interacts with genes involved in neural tube closure in mice including *Ptk7* (Lu et al., 2004), which is a receptor tyrosine kinase-like molecule involved in actin stress fiber formation in human umbilical vascular endothelial cells (Shin et al., 2008), *Dvl2* (Wang et al., 2006a), the actin-nucleating factor cordon-bleu (Carroll et al., 2003), and *circletail* (Murdoch et al., 2003), which is a mutant for *Scrb1*. Given the key role of Vangl2 in PCP signaling in other tissues, we set out to determine whether PCP effectors, specifically Vangl2, play a role in FRT development.

MATERIALS AND METHODS

Mouse breeding

Wnt7a and *loop-tail* mice were obtained from Jackson Labs (Bar Harbor, Maine, USA); *loop-tail* mice were maintained on a CBA background, and *Wnt7a* mice were bred to the *loop-tail* line for double-heterozygote analysis. Mice were housed under standard conditions with 12-hour light-dark cycles. *Wnt7a* genotyping was performed as described by Jackson Labs. Ovarectomized nude mice were obtained from Janvier (Le Genest St Isle, France). Grafting of FRT tissue in the renal capsule of ovariectomized nude mice was performed as described (Mericskay et al., 2004).

Histology and immunofluorescence

Grafts were dissected from nude host kidneys, placed in OCT and snap-frozen in isopentane chilled on dry ice. Sections (6-8 μm) were post-fixed for 10 minutes with 4% paraformaldehyde (PFA) in PBS, and stained with Hematoxylin and Eosin (H&E) or Oil Red using standard protocols. Phenotypic index data were obtained by blinding wild-type and mutant sections and scoring them from 1 to 4, with 1 being the lowest level for each phenotype. E18.5 FRTs were dissected from wild-type and mutant littermates obtained by C-section at day 18.5 of gestation. All tissues processed for immunofluorescence were embedded in OCT (Sakura, Netherlands), snap-frozen as described, and cryosectioned (5-7 μm). Immunostaining was performed on sections post-fixed for 20 minutes with 4% PFA in PBS, permeabilized using 0.2% Triton X-100 in PBS, blocked with 10% fetal calf or goat serum (Invitrogen, Carlsbad, CA, USA) plus 2% IgG-free BSA (Jackson ImmunoResearch, Newmarket, UK) and incubated with primary antibody overnight at 4°C. Antibodies were used at the following dilutions: Vangl2 (Montcouquiol et al., 2006b) 1:600, scribble (Santa Cruz, CA, USA) 1:400, E-cadherin (Zymed, San Francisco, CA, USA) 1:1200, smooth muscle actin (Sigma, St Louis, MO, USA) 1:400, ZO-1 (Santa Cruz Biotechnology, Santa Cruz, CA, USA) 1:400, Ki67 (BD Transduction Laboratories, Franklin Lanes, NJ, USA) 1:100, RhoA (Santa Cruz) 1:200, Magi3 (BD Transduction Laboratories). Secondary antibodies, conjugated with Alexa Fluor 488 or 568 (Invitrogen) or Cy3 (Jackson ImmunoResearch, West Grove, PA, USA) were used at 1:400. Cytoskeletal actin was labeled with Alexa 647-phalloidin (Invitrogen) at 1:150 in PBS for 45 minutes just before a 2-minute DAPI (0.5 mg/mL) stain. Slides were mounted with MolWiol or Prolong Gold anti-fade reagent (Invitrogen). Images were taken with a Leica SP2 confocal microscope and software, and collages were created in Adobe Photoshop CS2 by merging red, blue and green channels; adjustments to signal levels (except DAPI) were performed on the entire figure so as to ensure that panels were treated equally.

Quantitative reverse-transcriptase (RT) PCR

RNA was isolated from uterine horns (with ovaries removed) of individual animals using the RNeasy Micro Kit (Qiagen, Valencia, CA, USA) and cDNA prepared with the SuperScript First-Strand Synthesis System for RT-PCR using random primers (Invitrogen). For DES-exposed samples, DES (200 μg) was injected into pregnant mothers as described (Iguchi et al., 1986).

RT-PCR was performed on duplicate samples from at least three animals per genotype using the ABsolut SYBR Green ROX Mix (Thermo Fisher Scientific, Waltham, MA, USA) with the following primers (5′ to 3′): acidic ribosomal phosphoprotein (P0 control) forward CTCCAAGCAGATGCAGCAGA and reverse ATAGCCTTGCGCATCATGGT); Wnt7a forward GACAAATACAACGAGGCCGT and reverse GGCTGTCTTATTGCAGGCTC; Wnt5a forward CTCCTTCGCCCAGGTTGTTATAG and reverse TGTCTTCGCACCTTCTCCAATG; Wnt4 forward GAGAAGTGTGGCTGTGACCGG and reverse ATGTTGTCCGAGCATCCTGACC. Reactions were analyzed using a BioRad Opticon2. Calculations of change in expression relative to control were made using the ΔΔCt method.

RESULTS

At birth, *Vangl2^{Lp}* mutant female reproductive tracts display gross morphological and histological defects similar to those of *Wnt7a* mutants

E18.5 *Vangl2^{Lp}* mutant FRTs displayed several overt defects in their gross morphology as compared with wild-type FRTs (Fig. 1). There was a striking defect in the fusion of uterine horns at the level of the cervix (Fig. 1B,C), as previously described (Murdoch et al., 2001; Strong and Hollander, 1949). *Vangl2^{Lp}* mutant mice also lacked

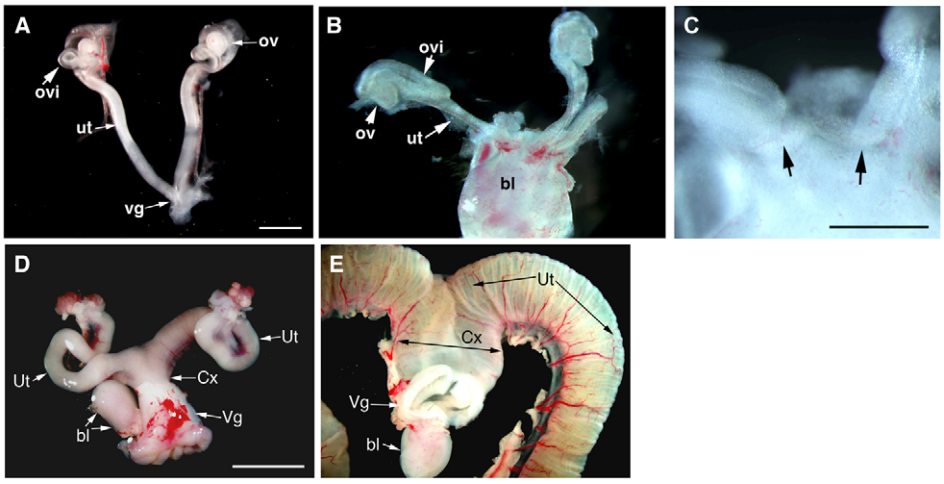

Fig. 1. *Vangl2*^{Lp} mutants have gross morphological defects at E18.5: ~50% of *Vangl2*^{Lp} heterozygote adult females are infertile and have a septate vagina. Wild-type (**A**) and *Vangl2*$^{Lp/Lp}$ mutant (**B**,**C**) E18.5 mouse female reproductive tract (FRT). The mutant demonstrates a lack of oviduct coiling and a septate vagina (arrows in C). (**D**) Wild-type adult FRT. (**E**) About 50% of *Vangl2*^{Lp} heterozygote FRTs are greatly enlarged and fluid-filled, indicating a vaginal blockage. ovi, oviduct; ov, ovary; ut, uterine horn; cx, cervix; vg, vagina; bl, bladder. Scale bars: 1 mm in A,B; 0.5 mm in C; 5 mm in D,E.

oviduct coiling (Fig. 1B) and uterine horns appeared shortened (Fig. 1B). We found that about half of the adult female heterozygous *Vangl2*^{Lp} mice were infertile; many exhibited an increased vaginal and anal opening space. As infertile females reached 4 to 6 months of age, approximately half displayed an enlarged abdomen owing to the presence of fluid-filled and grossly extended uterine horns (Fig. 1D). We noted, however, that the heterozygous *Vangl2*^{Lp} cervix and vagina appeared normal. In one case (n=3), the outer vaginal opening formed a blind pouch that did not connect to the internal reproductive organ (data not shown).

Plastic semi-thin sections taken from *Vangl2*^{Lp} mutant and wild-type littermate controls at E18.5 demonstrated several striking differences (Fig. 2A,B). First, *Vangl2*^{Lp} mutant uterine tissue displayed a disorganized cellular structure in comparison with wild-type littermates. Specifically, we observed differences in the orientation and organization of mesenchymal cells. Mesenchymal cells underlying the epithelium aligned their cell axes with the underlying epithelium (Fig. 2A,C), whereas mesenchymal cells in *Vangl2*^{Lp} mutant uteri were misaligned (Fig. 2B,D). We observed differences in the organization of the *Vangl2*^{Lp} mutant epithelium (Fig. 2B) and an overall rounder lumen (n=5), although the wild type does have a round lumen early in development. The edges of the epithelial cells facing the lumen appeared smoother and more closely packed together in the *Vangl2*^{Lp} mutant compared with the wild type.

Higher resolution examination of the *Vangl2*^{Lp} mutant epithelium using transmission electron microscopy (EM) revealed that the epithelium of mutant uteri (Fig. 2D) does not appear columnar as compared with the wild type (Fig. 2C). Instead, the mutant epithelium consisted of multiple cell layers and rounder nuclei. Although higher magnification did not reveal defects in either desmosomes or tight junctions per se, we observed electron-dense fibrillar-like structures in the area of the tight junctions of *Vangl2*^{Lp} mutant epithelium (Fig. 2F), in contrast to the situation in the wild type (Fig. 2E). These results prompted us to observe epithelial cell tight junction markers more closely.

E-cadherin staining reveals a defect in uterine epithelial morphology in *Vangl2*^{Lp} mutants

E-cadherin is expressed ubiquitously in epithelial cell types (Butz and Larue, 1995). E-cadherin localization appeared normal in *Vangl2*^{Lp} mutant epithelium as compared with wild type (Fig. 2G,H). However, as shown in Fig. 2I,J, we noted ectopic epithelial cell layers in the *Vangl2*^{Lp} image. In rare cases (n=3 images from two different mutants), these abnormal epithelial cells appeared to lose contact with neighboring cells and reside in the lumen (Fig. 2H, arrow). Generally, there were 2 to 4 layers of rounded epithelial cells in *Vangl2*^{Lp} mutant uteri, rather than the 1 to 2 layers of elongated columnar epithelial cells in the wild type. Given these changes in *Vangl2*^{Lp} mutant epithelium, it seemed possible that proliferation might be altered; however, immunofluorescence (IF) staining for the Ki67 (Mki67) proliferation marker revealed no significant differences between mutant and wild-type sections at E18.5 (data not shown).

Vangl2 protein localizes to the apical edges of epithelial cell membranes and to glands

We performed IF analysis on uterine sections using an antibody to the Vangl2 protein (Fig. 3) (Montcouquiol et al., 2006b). At E18.5, Vangl2 protein was found in uterine epithelial cells and appeared to be membrane localized and enriched at the lateral edges near the luminal apical edge of wild-type epithelial cells (Fig. 3A,C). In 1-month-old uterine samples, Vangl2 protein was localized throughout the entire periphery of the epithelial membrane, was concentrated at lateral cell edges and enriched at the apical portion of these cell-cell contacts (Fig. 3D,E). Also, Vangl2 protein localized to the cell membranes within glands (Fig. 3E), but with uniform distribution throughout the membrane. The same Vangl2 localization pattern was observed in reproductively mature 2-month-old adult uterine tissue, and in E18.5 vaginal epithelium (data not shown). As shown in Fig. 3B, almost undetectable levels of Vangl2 staining were observed in *Vangl2*^{Lp} mutants, consistent with previous observations (Montcouquiol et al., 2006b).

Vangl2^{Lp} mutant uteri display defects in cytoskeletal actin polarization

Given the gross morphological changes in *Vangl2*^{Lp} mutant uteri, and the demonstrated involvement of the Vangl2 protein in PCP, we undertook a molecular analysis of *Vangl2*^{Lp} mutants to characterize protein localization for known polarity markers and Vangl2-interacting proteins in the FRT. Phalloidin staining of filamentous cytoskeletal actin demonstrated that actin polarizes to the apical edges of epithelial cells in wild-type uteri at E18.5 (Fig. 4A,C), whereas in *Vangl2*^{Lp} mutants the polarization of cytoskeletal actin was markedly reduced (Fig. 4B,D). Serial examination of z-plane optical sections revealed gross cytoskeletal actin polarity defects throughout the section (compare Movie 1 with Movie 2 in the supplementary material). However, IF localization of Cdc42 and

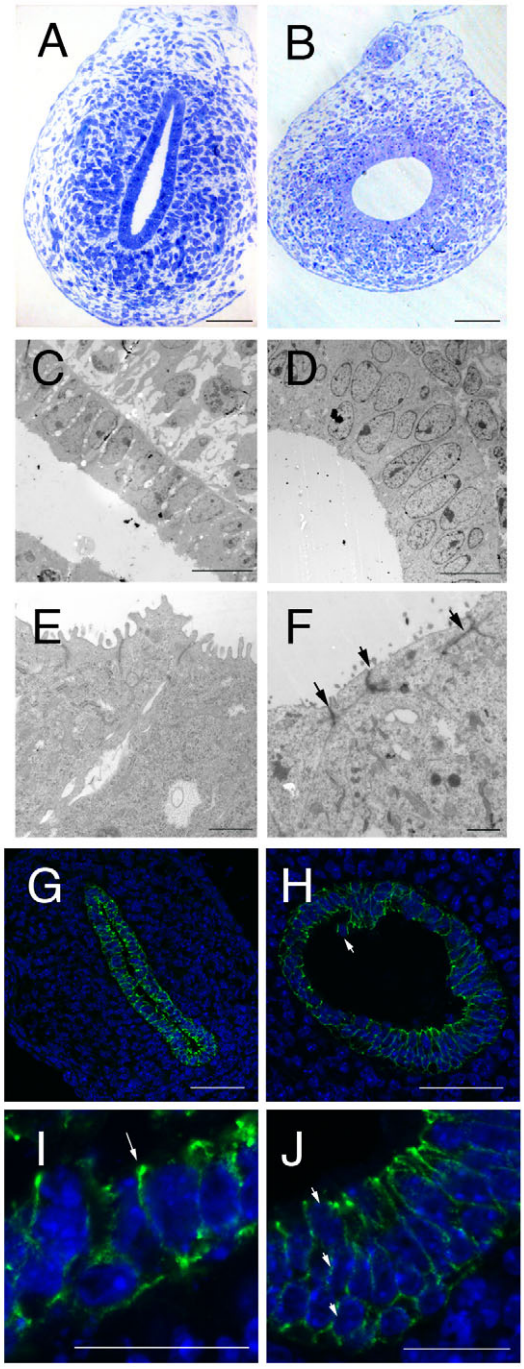

Fig. 2. *Vangl2*^{Lp} mutants display alterations in cytoarchitecture at E18.5, including the loss of typical columnar epithelial cell morphology. (**A**,**B**) Wild-type (A) and *Vangl2*^{Lp} mutant (B) mouse uterine semi-thin cross-sections reveal a change in uterine lumen shape in the mutant (it is more rounded) as well as disorganized mesenchyme and non-columnar epithelium. (**C-F**) Transmission EM of wild type (C,E) and *Vangl2*^{Lp} mutant (D,F) reveals ultrastructural changes associated with the loss of columnar uterine epithelial cell morphology in mutants. Near the tight junctions, electron-dense fibrillar structures are seen in the mutant (F, arrows), but are rarely visible in wild type (E). (**G-J**) Immunofluorescent confocal staining of E18.5 wild-type (G,I) and mutant (H,J) uterine sections with E-cadherin antibody. Note the nearly detached epithelial cell (H, arrow). E-cadherin is enriched at the apical edge (I, arrows); note increased number of cell layers of E-cadherin-staining epithelium in the *Vangl2*^{Lp} mutant (J, arrows). Scale bars: 10 μm in C,D,G,H; 5 μm in A,B,I,J; 1 μm in E,F.

RhoA proteins did not reveal any differences between the wild type and *Vangl2*^{Lp} mutant (data not shown), suggesting that the defect in cytoskeletal actin polarization is not due to any detectable defect in the localization of either of these polarity proteins.

Vangl2^{Lp} mutant epithelium has defects in scribble localization

Alterations in the morphology and cellular organization of mutant epithelium prompted us to further explore whether the integrity of cell-cell interactions was impaired in *Vangl2*^{Lp} mutants. IF localization was performed against the tight junction protein ZO-1. No differences were detected between mutant and wild type (data not shown). Scrb1 protein interacts with Vangl2 and this interaction can be detected by protein co-immunoprecipitation (Kallay et al., 2006; Montcouquiol et al., 2006a). IF localization on E18.5 uterine sections (Fig. 4E-H) revealed an accumulation of Scrb1 at the apical edges of *Vangl2*^{Lp} mutant epithelial cells (Fig. 4H) as compared with wild type (Fig. 4G), with an apparent increase in the intensity of Scrb1 staining in mutants. Scrb1 functions together with Lgl2 and Dlg to establish apical/basolateral polarity (Bilder et al., 2003; Humbert et al., 2003; Tanentzapf and Tepass, 2003) and is localized to the basolateral membrane of MDCK epithelial cells and human uterine cervical epithelial tissues (Nakagawa et al., 2004). This result suggests that Vangl2 protein is required to restrict Scrb1 to the basolateral domain of the uterine epithelial membrane.

Grafting to enable observation of postnatal development of *Vangl2*^{Lp} FRT

As *Vangl2*^{Lp} mutants die at birth, a grafting technique using ovariectomized nude mouse hosts was used to observe postnatal FRT development (Cunha, 1976a). Briefly, the grafting technique consists of placing fetal reproductive tissues under the renal capsule of the host nude mouse and then harvesting the grafted tissue at various time points. Our previous studies show that 2 weeks is sufficient time to obtain completely normal tissue architecture when grown in ovariectomized hosts, while avoiding precocious estrogen exposure during reconstitution of the tissue and cellular morphology (Mericskay et al., 2004). As expected, wild-type E18.5 tissue developed all of the normal histological features of wild-type FRT in situ, including glands and smooth muscle. By contrast, grafts of mutant tissue generated all the proper cell types but showed an overall exacerbation of the disorganized phenotype seen at birth (Fig. 5). The histological defects seen in *Vangl2*^{Lp} heterozygote and mutant grafted uterine tissue were generally an exacerbation of the phenotype observed at E18.5 (Fig. 2). Specifically, the epithelium became highly pseudostratified, and other unusual epithelial morphologies were present in both *Vangl2*^{Lp} heterozygotes (Fig. 5C-H) and homozygotes (Fig. 5I-N) that were not present in wild-type grafts (Fig. 5A,B). Acellular material accumulated in the lumen of a *Vangl2*^{Lp} heterozygote (Fig. 5C,D). We also observed pseudostratified epithelium (Fig. 5F,H) with a large band of Eosin-stained material towards the basolateral cell edge (compare Fig. 5F with 5B). What appeared to be cell protrusions into the lumen were occasionally seen at high magnification in *Vangl2*^{Lp} heterozygous (Fig. 5H) and homozygous (data not shown) mutants. An increase in the number and size of lipid-like vesicles or vacuoles was noticeable in homozygous (Fig. 5J) and heterozygous (Fig. 5F,H) mutants. Only some of these vesicles stained positively with Oil Red O (data not shown), suggesting that they are not composed entirely of lipid vesicles. Finally, regions of epithelium that appeared hyperpolarized were observed in homozygous mutants (Fig. 5K,L). Delaminated epithelial cells were observed in two of four

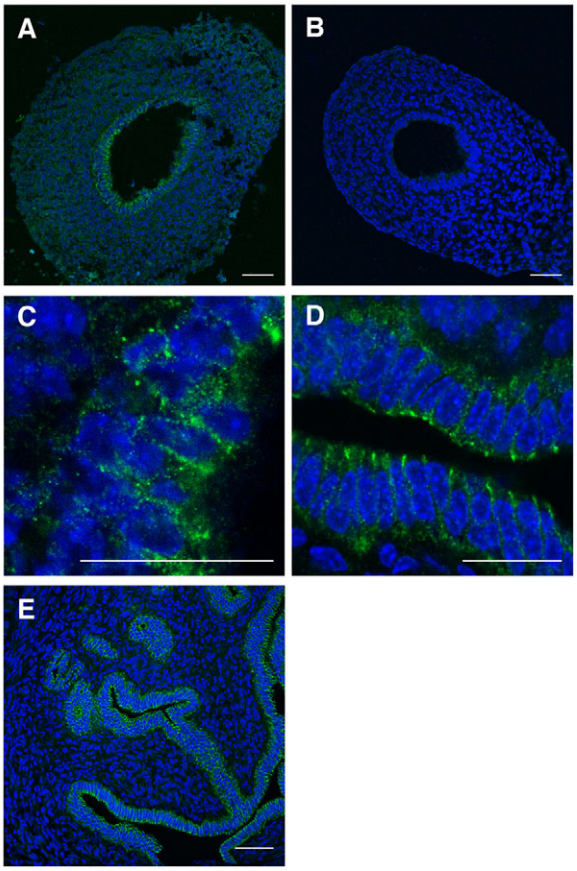

Fig. 3. Vangl2 protein localizes to epithelial membranes and is enriched at the apical edge of lateral cell contacts in both immature and adult uterus. In E18.5 wild-type mouse uterine tissue, Vangl2 protein (green), as detected by confocal IF, localizes to epithelial cell membranes (**A**) and is enriched at cell junctions (**C**), whereas in the *Vangl2*^{Lp} mutant at E18.5 (**B**) there is very little detectable expression. In 1-month-old wild-type tissue, Vangl2 is enriched at the apical edge of lateral cell contacts (**D**) and is similarly found at epithelial cell membranes (**E**) and in the epithelium of glands. We note that the wild type shown here (A) has a somewhat rounder lumen, reflecting the fact that it was harvested at a slightly earlier stage than E18.5 to allow for easier visualization of the IF staining. Scale bars: 50 μm in A,B; 5 μm in C,D; 10 μm in E.

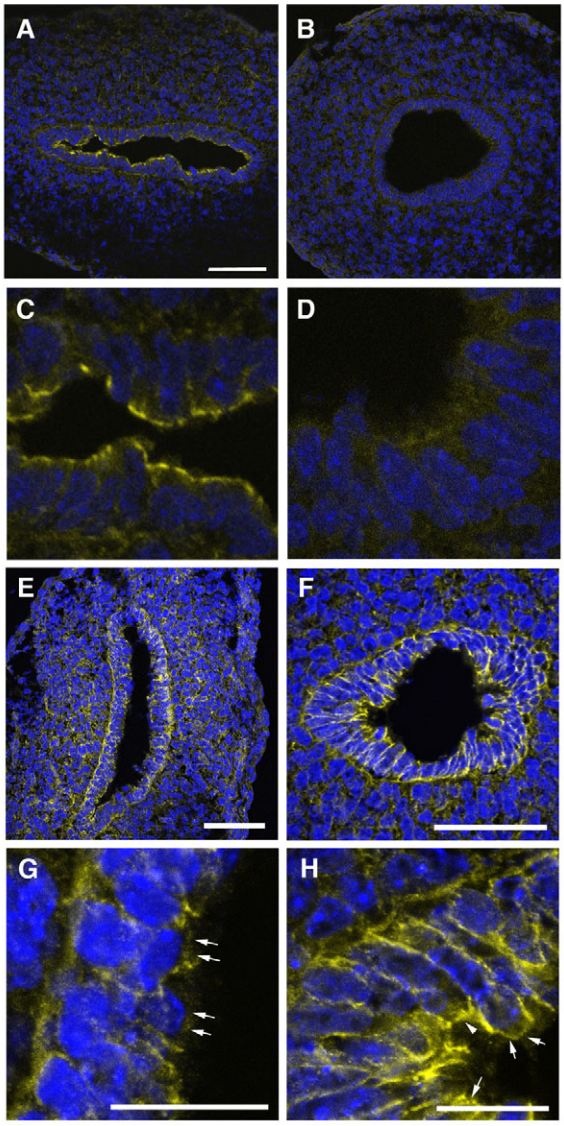

Fig. 4. *Vangl2*^{Lp} mutants have defective cytoskeletal actin polarization and scribble distribution is not restricted to the apical edge of epithelial cells at E18.5. (**A-D**) Wild-type (A,C) and *Vangl2*$^{Lp/Lp}$ mutant (B,D) mouse uterine sections were stained with Alexa 647-phalloidin. C,D are higher magnifications from A,B, with the lumen located towards the upper left in D. (**E-H**) Scrb1-stained (yellow) uterine sections of wild type (E,G), and *Vangl2*$^{Lp/Lp}$ mutant (F,H) with the lumen located to the right in G,H. Arrows delineate the apical edge (G,H), which displays increased Scrb1 signal in the *Vangl2*^{Lp} mutant (H). Scale bars: 10 μm in A,B,E,F; 5 μm in G,H.

independent grafts (Fig. 5M,N). To assess the overall phenotypic changes observed in H&E-stained grafts, a qualitative analysis was performed on blinded tissue sections (Table 1). We concluded that *Vangl2*^{Lp} heterozygotes demonstrate minor changes in pseudostratification and in epithelial vesicles compared with wild-type grafts. *Vangl2*^{Lp} mutants, however, had a markedly increased index of pseudostratification (2.8) and epithelial vesicles (2.0) compared with the wild type (1.3 for both categories). Both heterozygous and homozygous *Vangl2*^{Lp} mutants displayed a drastic reduction in total mesenchyme and increase in smooth muscle (Table 1), as observed by H&E staining.

Postnatal grafts of *Vangl2*^{Lp} FRT have altered F-actin, E-cadherin, scribble and smooth muscle actin staining

IF staining of uterine tissue grafted for 2 weeks demonstrated abnormal localization of polarity markers. Filamentous actin is normally localized as a faint band of membrane staining at the apical edge of wild-type epithelial cells (Fig. 6B). In *Vangl2*^{Lp} homozygous mutant grafts, stronger actin staining was apparent, which extended to adjacent cells (Fig. 6E) rather than being localized to apical membranes directly adjacent to the lumen. Filamentous actin staining was evident around the entire cell periphery in some epithelial cells of homozygous mutants (see Fig. 6E, arrows) and was uneven in intensity. The E-cadherin localization pattern was also altered in *Vangl2*^{Lp} mutants (Fig. 6F). In wild-type grafts and in postnatal tissue (data not shown), E-cadherin was membrane localized and enriched at apical cell edges and lateral cell-cell contacts towards the apical edge (Fig. 6C, arrows), whereas

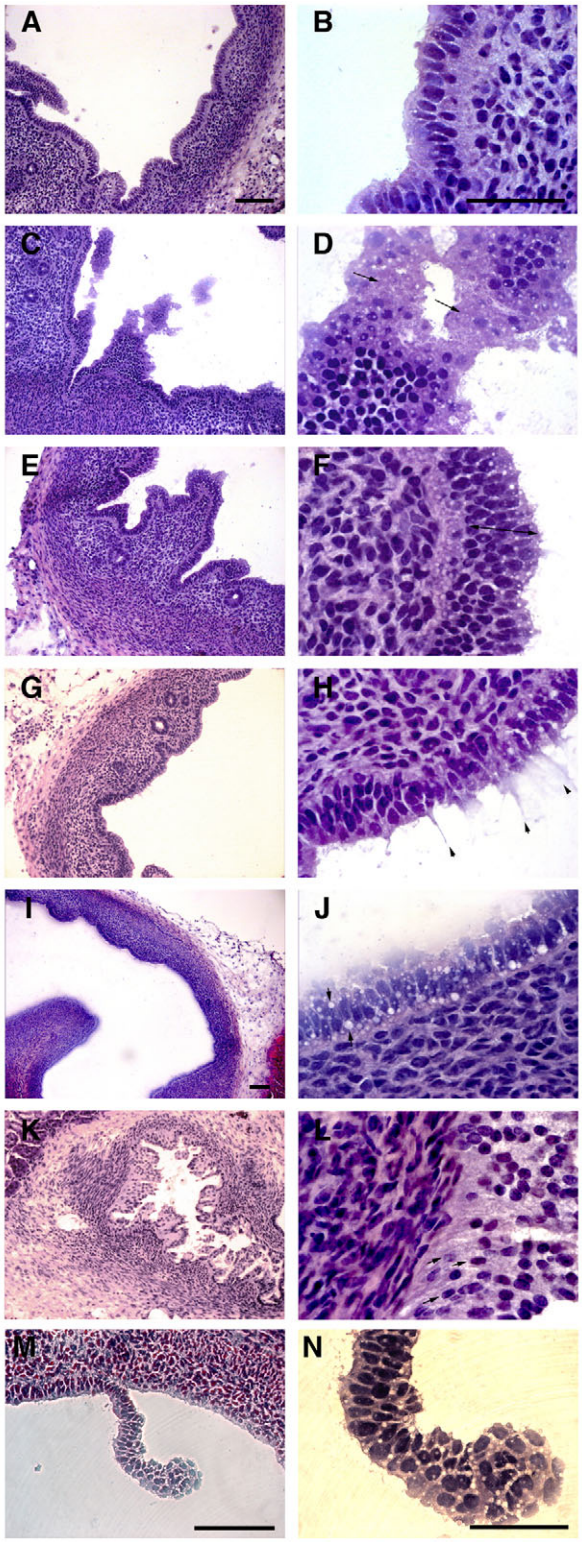

Fig. 5. Heterozygous and homozygous *Vangl2^{Lp}* mutant grafted postnatal uterine tissues demonstrate various histological abnormalities, especially in the epithelium. Wild-type (**A**,**B**), *Vangl2$^{Lp/+}$* (**C-H**) and *Vangl2$^{Lp/Lp}$* mutant (**I-N**) mouse tissues were grafted in the kidney capsule of ovarectomized nude mice for 2 weeks, cryosectioned and H&E stained. Bright-field images are shown. Images in the right-hand column are magnifications of those in the left column. Arrows indicate acellular material (D). Note the presence of glands in wild type (A,C) and heterozygous mutant (E,G). The double-headed arrow in F indicates the expanded layer of pseudostratified epithelium. Arrows in H indicate cell projections. Note the increased number and size of lipid droplets or vacuoles (J, arrows), the presence of cells that appear hyperpolarized (L), and epithelial cells that have detached from the underlying mesenchyme (N). Scale bars: 10 μm in A,C,E,G,I,K,M; 5 μm in B,D,F,H,J,L,N.

Vangl2^{Lp} mutants had uneven E-cadherin staining and had lost the E-cadherin enrichment at regions of cell-cell contact (Fig. 6F, arrows). Colocalization analysis of these markers demonstrated that filamentous actin has a more limited apical expression domain than E-cadherin in wild type (Fig. 6A), whereas in *Vangl2^{Lp}* mutants the actin and E-cadherin staining overlapped (Fig. 6D).

Scrb1 distribution was perturbed in postnatal grafted heterozygous and homozygous *Vangl2^{Lp}* mutant tissue. In the wild type, Scrb1 was localized predominantly to regions where epithelial cells invaginate (Fig. 6G) and to puncta at cell-cell contacts where tight junctions are located (Fig. 6J), adjacent to regions that stained strongly for Vangl2 localization (Fig. 3D,E), consistent with previous observations that Scrb1 binds Vangl2 (Kallay et al., 2006; Montcouquiol et al., 2003). By contrast, the entire multi-layered population of pseudostratified heterozygous (Fig. 6H,K) and homozygous (Fig. 6I,L) *Vangl2^{Lp}* mutant epithelium stained the entire membrane more strongly than in wild type (Fig. 6G,J). Apically located heterozygous and homozygous mutant epithelial cells had increased Scrb1 at cell-cell contacts (Fig. 6H,I,L) and the expression domain was larger than in the wild type (Fig. 6J, arrow); in the underlying layers of mutant epithelial cells, Scrb1 was uniformly localized throughout the entire cell membrane (Fig. 6H,I,L).

H&E staining of grafts showed an increase in smooth muscle in postnatal grafted *Vangl2^{Lp}* tissue (Fig. 5; Table 1). IF confirmed that smooth muscle actin-stained tissue was increased in postnatal grafted heterozygous (Fig. 6N) and homozygous (Fig. 6O) *Vangl2^{Lp}* mutant tissue, as compared with wild type (Fig. 6M), with a corresponding decrease in total mesenchyme (double-headed arrows in Fig. 6M,N; arrowheads in Fig. 6O).

Vangl2^{Lp} mutant uteri have reduced *Wnt7a* expression

Several Wnt signaling members function in FRT development and, given the similarities in gross morphology between *Vangl2^{Lp}* mutants and *Wnt7a* mutants, we measured the expression of several Wnt genes using quantitative RT-PCR at E18.5 (Fig. 7). Both heterozygous and homozygous *Vangl2^{Lp}* mutants displayed a significant reduction in *Wnt7a* (Fig. 7A). Diethylstilbestrol (DES) downregulates *Wnt7a* expression as previously described (Mericskay et al., 2004; Miller and Sassoon, 1998). We observed that DES reduced *Wnt7a* transcription to very low levels: 9% of wild type, compared with a 52-60% reduction in *Vangl2^{Lp}* mutants. This suggests that the *Vangl2^{Lp}* mutation partially perturbed *Wnt7a* expression. Neither *Wnt5a* nor *Wnt4* expression was altered in either heterozygous or homozygous *Vangl2^{Lp}* mutants (Fig. 7B,C). However, perinatal DES exposure notably altered *Wnt4* and *Wnt5a* expression as expected. This result suggests that the moderate disruption of *Wnt7a* expression in *Vangl2^{Lp}* heterozygous and homozygous mutants was not sufficient to alter expression of the other Wnt genes in neonatal tissues.

Table 1. Phenotypic characterization of postnatal grafted tissue

Genotype	Glands	Pseudostratified	Vesicles	Mesenchyme to muscle	Cell protrusions
WT	4	1	1	>>	–
WT	14	2	2		–
WT	1	1	1	=	–
Average	6.3	1.3	1.3	n.d.	
Lp/+	0	2	3	=	++
Lp/+	10	2	0	n.a.	–
Lp/+	3	1	1	<	–
Lp/+	3	2	2	<	–
Lp/+	1	2	2	<<<	–
Lp/+	0	2	0	<<<	–
Lp/+	0	3	3	=	–
Lp/+	0	2	2	n.a.	–
Lp/+	0	0	0	<<<	–
Lp/+	0	1	1	<<	–
Lp/+	0	2	1	=	–
Lp/+	4	1	1	n.a.	–
Average	1.8	1.6	1.3	n.d.	
Lp/Lp	3	4	3	<<<	–
Lp/Lp	2	3	1	<	–
Lp/Lp	10	3	3	<	++
Lp/Lp	8	3	0	<<<	–
Lp/Lp	2	3	2	<<	–
Lp/Lp	1	2	3	n.a.	–
Lp/Lp	4	2	2	<	++
Average	4.3	2.8	2.0	n.d.	

Vangl2^{Lp} mutant grafts have an increased index of abnormal phenotypes as observed by H&E staining. Column headings refer to histological phenotypes observed by microscopic observation of the entire section of H&E-stained grafted tissue and designate the following: Glands, the total number of glands; Pseudostratified, the degree of pseudostratified epithelium; Vesicles, lipid vesicles or vacuoles of increased size and/or number; Mesenchyme to muscle, the proportion of total mesenchyme versus total muscle (> indicates more mesenchyme than muscle); Cell protrusions, epithelial cell protrusions or extensions projecting into the lumen. The phenotypic index was determined by calculating the average value for each genotype as shown in the 'average' row.
Lp, *Vangl2*^{Lp} mutation; WT, wild type; n.a., not applicable; n.d., not done.

Genetic interactions between *Vangl2*^{Lp} and *Wnt7a*

When *Wnt7a* heterozygote females were crossed to *Wnt7a*$^{+/-}$; *Vangl2*$^{Lp/+}$ double heterozygotes we observed a genetic interaction between the *Vangl2*^{Lp} and *Wnt7a* alleles (Table 2). The expected ratio of *Vangl2*$^{Lp/+}$; *Wnt7a*$^{-/-}$ offspring is 12.5%, whereas we obtained 3.3% of mice with this genotype, suggesting either a semi-lethal interaction when one allele of *Vangl2*^{Lp} is in the context of a homozygous *Wnt7a* mutation, or an enhancement of the *Vangl2*^{Lp} phenotype in the *Wnt7a* mutant background. There was a gender bias with double-heterozygous offspring: 11.3% females and 42.1% males were obtained, versus an expected ratio of 25%. This suggests that male pups might have reduced lethality.

DISCUSSION

Morphological defects of *Vangl2*^{Lp} mutants partially overlap with those of *Wnt7a* mutants

We observe phenotypic overlap among *Wnt7a* and *Vangl2*^{Lp} mutants, consistent with observations that *Wnt7a* levels are lower in *Vangl2*^{Lp} mutants. Nonetheless, a partial decrease in *Wnt7a* expression in *Vangl2*^{Lp} mutants cannot explain all of the gross morphological defects observed. The uterine horns of *Vangl2*^{Lp} mutants fail to fuse at the cervix, as previously described (Strong and Hollander, 1949), and oviduct coiling is lacking, similar to what we and others observe in *Wnt7a* mutants (Miller et al., 1998a; Miller and Sassoon, 1998; Parr and McMahon, 1998). However, other phenotypes observed suggest that additional pathways are affected in *Vangl2*^{Lp} mutants. Uterine horns appear shortened in *Vangl2*^{Lp} mutants, consistent with a role in convergent extension and rostral-caudal lengthening, as observed in shortened *Xenopus* embryos with a loss-of-function in Trilobite (homolog of Van Gogh) (Darken et al., 2002; Goto and Keller, 2002; Jessen et al., 2002; Park and Moon, 2002), as well as the shorter temporal bones and cochlea in *Vangl2*^{Lp} mice (Montcouquiol et al., 2003). Although the uterine horns of *Wnt7a* mutants are smaller in diameter (Miller and Sassoon, 1998), this defect is not found in *Vangl2*^{Lp} mutants. *Wnt7a* heterozygous uterine tissues that most closely resemble the partial decrease in *Wnt7a* expression observed in *Vangl2*^{Lp} mutants display increased gland formation in the postnatal uterus (Miller and Sassoon, 1998), but they display neither the epithelial pseudostratification nor the increase in smooth muscle observed in *Vangl2*^{Lp} mutants.

We observe semi-penetrant infertility of *Vangl2*^{Lp} heterozygotes, whereas *Wnt7a* heterozygotes are fertile. The uterine block observed in *Vangl2*^{Lp} adult heterozygotes is not due to the septation observed in *Wnt7a* mutants, consistent with distinct *Vangl2*^{Lp} and *Wnt7a* mechanisms. The uterine blockage accompanied by the lack of a proper vagina closely resembles vaginal agenesis, which is present in ~1/5000 human births. This can be accompanied by painful symptoms if endometrial uterine tissue remains, as it does in ~7-10% of cases (Rackow and Arici, 2007). Therefore, Vangl2 is a candidate gene for vaginal agenesis in humans.

Changes in the cell polarity of neonatal reproductive tissues have lasting consequences for female reproductive tract development

Histological, EM and IF examination of *Vangl2*^{Lp} mutants reveal numerous defects in the cellular organization of neonatal *Vangl2*^{Lp} mutants. Mesenchymal cells adjacent to the epithelium align their cell axes with the underlying epithelium, whereas mesenchymal

Table 2. Ratio of pups obtained from *Wnt7a* and *Vangl2*^{Lp} crosses

Number of mice	Progeny	WT; WT	*Vangl2*$^{Lp/+}$	*Wnt7*$^{+/-}$	*Wnt7*$^{-/-}$	*Vangl2*$^{Lp/+}$; *Wnt7*$^{-/-}$	*Vangl2*$^{Lp/+}$; *Wnt7*$^{+/-}$
53	Female	16	0	22	6	3	6
38	Male	7	0	12	3	0	16
91	Total	23	0	34	9	3	22
	% Female	30.2	0.0	41.5	11.3	5.7	11.3
	% Male	18.4	0.0	31.6	7.9	0.0	42.1
	% Total	25.3	0.0	37.4	9.9	3.3	24.2
	% Expected	12.5	12.5	25.0	12.5	12.5	25.0
	% Difference	–12.8	12.5	–12.4	2.6	9.2	0.8

Wnt7a$^{+/-}$ females were crossed to *Wnt7a*$^{+/-}$; *Vangl2*$^{Lp/+}$ double heterozygotes. Expected Mendelian ratios are given in the penultimate row. χ^2<0.01.
Lp, the *Vangl2*^{Lp} mutation; WT, wild type; *Wnt7* is *Wnt7a*.

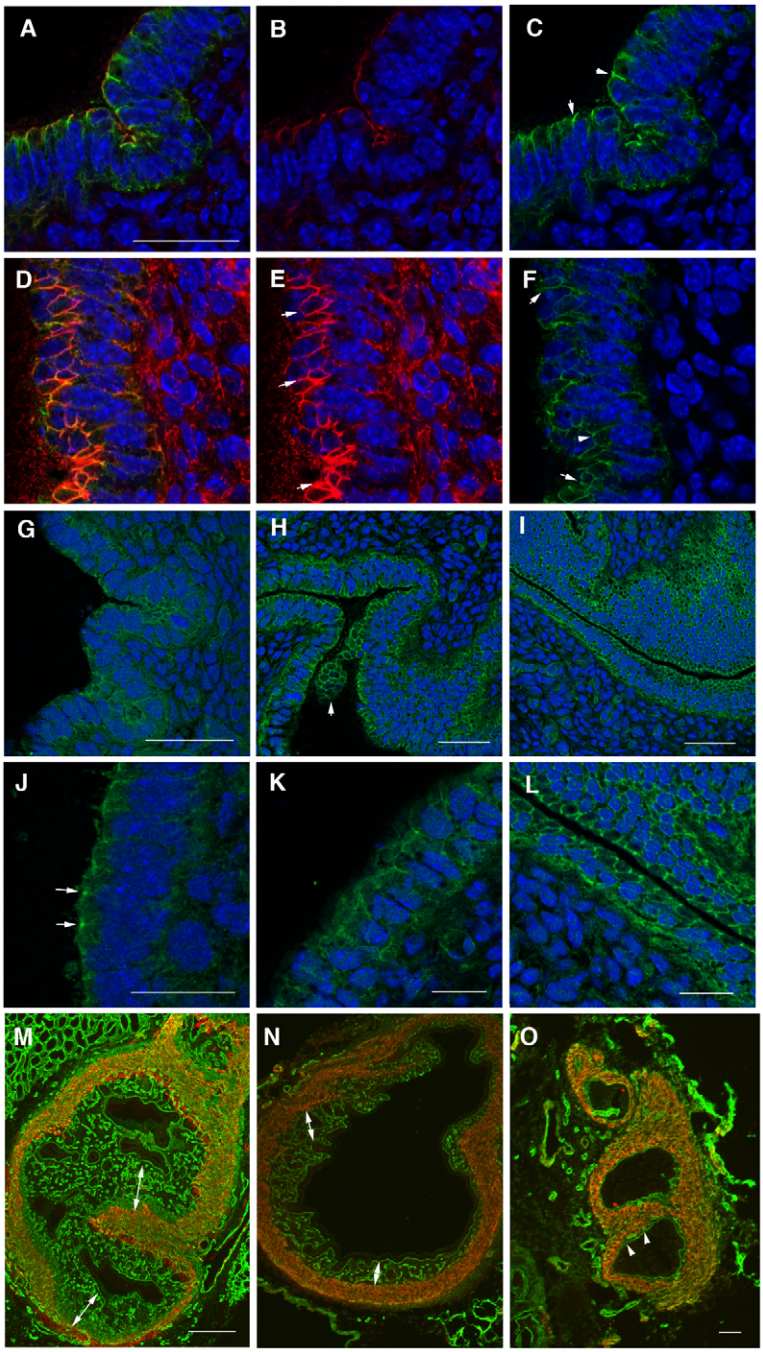

Fig. 6. Mutant *Vangl2*^{Lp} grafted postnatal uterine tissue displays hyperpolarized actin and abnormal E-cadherin distribution. (**A-F**) The wild type (A-C) has a thin and even domain of actin polarization towards the lumen, as compared with the *Vangl2*^{Lp} mutant (D-F) in which the actin staining (red) is uneven (compare B with E, arrows). E-cadherin (green) is enriched at the apical domain of lateral cell junctions in wild-type epithelium (C, arrows), but this localization is lost in the mutant (F, arrows). (**G-L**) Scrb1 localization is perturbed in grafted postnatal *Vangl2*^{Lp} mutant uterine tissue. The wild type (G,J) demonstrates discrete points of Scrb1 localization (green) to apical regions (lumen to the left in G,J) of epithelial cell-cell contact (J, arrows). By contrast, in *Vangl2*^{Lp} heterozygotes (H,K,I,L), the expanded pseudostratified layer of epithelial cells localize Scrb1 in a non-polarized fashion, including some Scrb1^{+} epithelial cells in the middle of the lumen (H, arrowhead) and uniform membrane localization (H,I,K,L). Scrb1 localization is abnormal in the highly pseudostratified *Vangl2*$^{Lp/Lp}$ mutant epithelium (I,L). (**M-O**) Increase in smooth muscle layer with corresponding decrease in number of mesenchymal cells in *Vangl2*^{Lp} mutants. Wild type (M), *Vangl2*$^{Lp/+}$ (N) and *Vangl2*$^{Lp/Lp}$ (O) grafted mouse uterine postnatal tissue sections were stained for laminin (green) and smooth muscle actin (red). Laminin delineates the basal lamina at the border between epithelium and mesenchyme. Double-headed arrows indicate the width of the mesenchyme (M,N). The homozygous mutant (O) displays smooth muscle directly adjacent to the basal lamina (no mesenchyme). Scale bars: 10 μm in G-I,M-O; 5 μm in A-F,J-L.

cells in *Vangl2*^{Lp} uteri are misaligned, similar to *Wnt7a* mutant uteri (Miller et al., 1998a; Miller and Sassoon, 1998). The loss of normal columnar epithelium in *Vangl2*^{Lp} uteri at birth and the rounded lumen are features unique to these mutants. Changes in uterine elasticity due to altered cell-cell contacts or loss of cell rigidity could explain the changes in the lumen shape of *Vangl2*^{Lp} mutants.

A reduction in polarized filamentous cytoskeletal actin was seen in neonatal *Vangl2*^{Lp} mutant epithelium as compared with wild type. Defects in polarized cell movement are observed in *Vangl2*^{Lp} mutant embryonic heart (Phillips et al., 2005), as well as actin cytoskeletal defects in mutant myocardial cells (Phillips et al., 2008). Hair follicles within *Vangl2*^{Lp} mutant epithelium fail to polarize and mislocalize a number of cellular markers, including E-cadherin and Celsr1 [homolog of *Drosophila* Flamingo (Starry night)] (Devenport and Fuchs, 2008). In postnatal *Vangl2*^{Lp} mutant uterine grafts, cytoskeletal actin staining becomes uneven and the protein is more strongly expressed in a wider domain than in wild-type epithelium. These data suggest that cytoskeletal remodeling events are important for early uterine patterning.

There is ample evidence that Scrb1 and Vangl2 interact in other murine tissues. Scrb1 interacts with Vangl2 as determined by protein co-immunoprecipitation (Kallay et al., 2006; Montcouquiol et al., 2006a), and mice mutant for *Scrb1* mislocalize Vangl2 in the hair cells of the cochlea (Montcouquiol et al., 2006b). Also, mutants of *Vangl2*^{Lp} or *Scrb1* demonstrate the same cardiac development defects as double heterozygotes, suggesting that Vangl2 and Scrb1 act in the same developmental pathway in the heart (Phillips et al., 2007). We observe Scrb1 localized to the apical edges of *Vangl2*^{Lp}

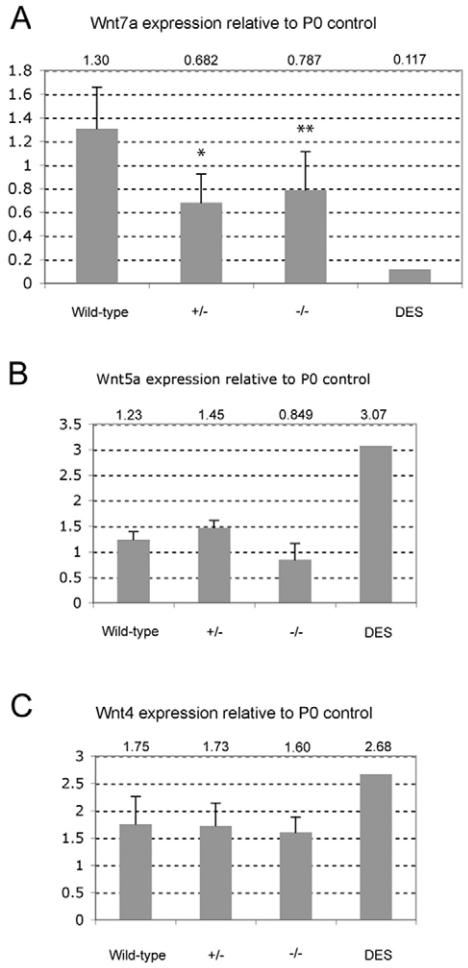

Fig. 7. *Wnt7a* expression is reduced in both heterozygous and homozygous *Vangl2^{Lp}* mutants. *Wnt7a* (**A**), *Wnt5a* (**B**) and *Wnt4* (**C**) expression was measured relative to P0 (acidic ribosomal phosphoprotein) control gene by quantitative RT-PCR of cDNA obtained from total RNA of mouse uterine horns from different animals. Error bars indicate s.d. of the mean; *P*-values were calculated using Student's *t*-test (wild type, n=3; *Vangl2$^{Lp/+}$*, n=3; *Vangl2$^{Lp/Lp}$*, n=5): **P*=0.873, ***P*=0.837.

mutant neonatal epithelium, suggesting that the domain of Scrb1 expression is expanded when the *Vangl2^{Lp}* mutation is present. Murine Scrb1 is basolaterally localized in MDCK cells (Nagasaka et al., 2006) and human SCRB1 is similarly localized in human uterine cervical epithelial tissues (Nakagawa et al., 2004). Scrb1 also functions in apical/basolateral cell polarity with Lgl2 and Dlg by antagonizing the activity of the apically localized Par complex (Bilder et al., 2003; Macara, 2004; Tanentzapf and Tepass, 2003). We propose that the *Vangl2^{Lp}* mutation provokes disruption of Scrb1 localization and that Scrb1 is no longer restricted to the basolateral domain of epithelial cells. Scrb1 has been shown to interact with Lgl2 as well as with Vangl2, and the analysis of macromolecular complexes containing Scrb1 have suggested that it organizes the intracellular face of the lateral plasma membrane by acting as a 'retaining wall' (Kallay et al., 2006). The fibrillar-like structures seen at the cellular junctions of *Vangl2^{Lp}* mutants in EM might result from an abnormal accumulation of proteins due to the presence of Scrb1 at the apical cell edge. Scrb1 expression in the FRT is dynamic. In postnatal grafted tissue, Scrb1 localization becomes concentrated at cellular junctions. This dynamic localization might reflect multiple roles for Scrb1, as it is essential for directed epithelial cell migration (Dow et al., 2007; Ludford-Menting et al., 2005; Qin et al., 2005). These data suggest a model in which Vangl2 and Scrb1 function together in a complex, and Vangl2 is required to restrict Scrb1 to the basolateral domain in neonatal uterine epithelial cells and to concentrate Scrb1 expression at areas of cell-cell contact in postnatal epithelial cells (Fig. 8).

E-cadherin is an epithelial marker (Butz and Larue, 1995) and interacts with β-catenin to promote cell junction adhesion (Gumbiner, 1997). E-cadherin interacts with scribble (Navarro et al., 2005; Qin et al., 2005). Whereas neonatal *Vangl2^{Lp}* mutant epithelium loses normal columnar morphology, it retains normal E-cadherin localization; however, polarity defects of mutant tissues become marked in postnatal tissues. In addition to defects in polarized filamentous actin and Scrb1 localization, we observe an increased domain of E-cadherin expression in *Vangl2^{Lp}* mutant epithelium. This increase in E-cadherin expression, coupled with an increase in the domain of Scrb1 expression, might alter the integrity of cellular junctions in postnatal tissues. When spindle pole orientation is perpendicular to the basement membrane in mouse skin, the epithelium becomes stratified rather than columnar (Lechler and Fuchs, 2005), supporting a model whereby cell division perpendicular to the basement membrane directs stratification. In this context, we observe changes in the alignment of cell axes in both *Wnt7a* and *Vangl2^{Lp}* mutant epithelium and in the underlying mesenchymal cells. *Wnt7a* mutants also display altered epithelial cell morphology, becoming stratified in reproductively mature adult female uterine tissues. However, *Wnt7a* mutants lack glands, whereas *Vangl2^{Lp}* mutant grafts form glands, highlighting another unique feature of *Vangl2^{Lp}* mutants. Taken together, these data suggest that *Wnt7a* and *Vangl2^{Lp}* mutant phenotypes are partially overlapping and that early changes in cell polarity of neonatal FRT can be linked to the ultimate pseudostratification of the *Vangl2^{Lp}* postnatal mutant epithelium.

In postnatal *Vangl2^{Lp}* mutant tissues, defects in the localization of Scrb1, E-cadherin and polarized filamentous cytoskeletal actin become more pronounced, suggesting that defects observed in neonatal undifferentiated FRT tissues have permanent effects upon postnatal development. Both the homozygous and heterozygous *Vangl2^{Lp}* mutant postnatal grafts exhibit a range of histological defects. Characterization with molecular markers demonstrates uneven, and occasionally massively increased, cytoskeletal actin staining, an increased and abnormal domain of E-cadherin expression in epithelial cells, the loss of specific Scrb1 localization to regions of cell-cell contact, and an increased domain of Scrb1 expression. These changes appear sufficient to alter the developmental program of the FRT.

The *Vangl2^{Lp}* mutation provokes a reduction of *Wnt7a* expression in female reproductive tissues

There is precedence for a hierarchical regulation of Wnt proteins in the FRT (Mericskay et al., 2004; Miller et al., 1998b; Miller and Sassoon, 1998), as well as in other tissues such as muscle (Tajbakhsh et al., 1998). Loss of Wnt7a provokes the misexpression of *Wnt5a* in mesenchyme and epithelium and leads to its eventual complete loss in adult tissues, and provokes the loss of *Wnt4* expression in the mesenchyme (Miller and Sassoon, 1998). Also, *Wnt5a* mutants have reduced *Wnt4* expression (Mericskay et al., 2004). This suggests that in general, the loss of Wnt signaling affects the expression of other Wnts in the developing FRT. Since the *Vangl2^{Lp}* mutation affects the expression of *Wnt7a*, which is also expressed in epithelium, this

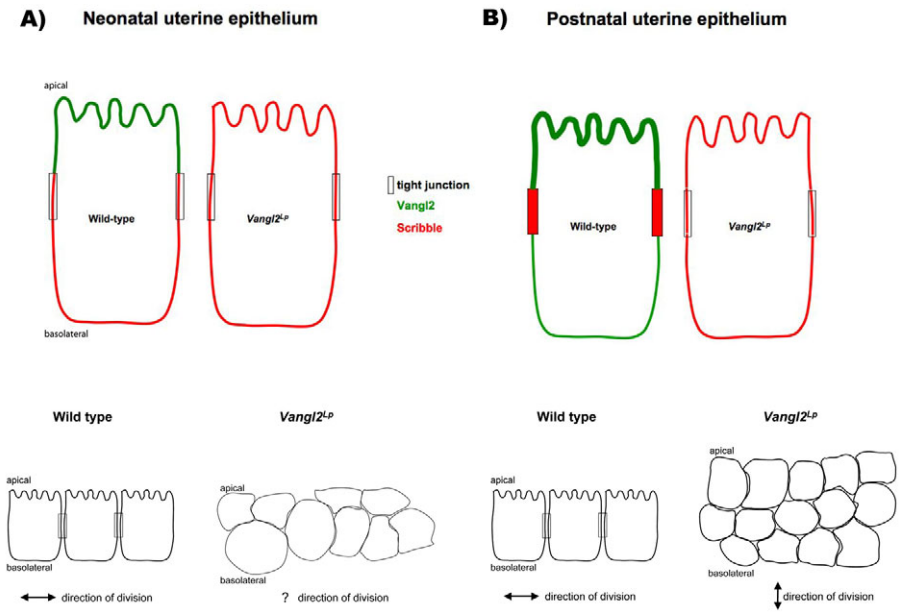

Fig. 8. Model showing how the *Vangl2*^{Lp} mutation functions in neonatal and postnatal female reproductive tissues. (**A**) Wild-type neonatal mouse uterine epithelium localizes Vangl2 protein in the apical domain and Scrb1 in the basolateral domain. When *Vangl2*^{Lp} is mutated, Scrb1 is no longer restricted to the basolateral domain. Wild-type epithelium remains columnar (beneath), whereas *Vangl2*^{Lp} mutant epithelium is no longer columnar. (**B**) In postnatal uterine epithelium, Vangl2 is still membraneous, but is enriched at the apical domain, whereas Scrb1 is concentrated at discrete puncta near tight junctions. Wild-type postnatal epithelium remains columnar (beneath), whereas in the *Vangl2*^{Lp} mutant it becomes highly pseudostratified, indicative of a change in the plane of cell division.

suggests that the mutation causes a disruption of Wnt signaling in the epithelium, which is nonetheless mild compared with signaling disruption by DES. DES, an estrogenic compound known to disrupt *Wnt7a* expression (Ma and Sassoon, 2006; Miller et al., 1998a), perturbs the expression of three Wnts – *Wnt7a*, *Wnt5a* and *Wnt4* – in neonatal FRT.

Three pieces of evidence support a model in which the *Vangl2*^{Lp} mutation acts in a dominant manner in the developing FRT. First, both heterozygous and homozygous *Vangl2*^{Lp} mutants show an almost identical decrease in *Wnt7a* expression. Second, the presence of either one or two copies of mutant *Vangl2*^{Lp} provokes similar changes in postnatal grafted FRT tissues, as observed by H&E, actin, E-cadherin and Scrb1 staining. Finally, we obtained fewer *Vangl2*$^{Lp/+}$; *Wnt7a*$^{-/-}$ compound mutant mice than expected. However, we cannot rule out the possibility that the *Vangl2*^{Lp} allele might cause increased lethality in the *Wnt7a* mutant background, as we obtain more *Wnt7a* heterozygous mice than the expected ratio (37.4% versus 25%) and fewer *Vangl2*^{Lp} heterozygous mice than expected (0% versus 12.5%). Taken together, these three lines of evidence suggest that the *Vangl2*^{Lp} mutation acts in a dominant manner in the developing FRT (Fig. 8). Finally, our results reveal that both the canonical and non-canonical pathways participate in FRT development and play a key role in maintaining and governing adult FRT function. Perturbations in the levels of Wnt ligands and/or their pathway effectors have profound effects upon reproductive function and tissue integrity.

We thank Jeanne Lainé MD, PhD, for the transmission electron images and the UMRS 582 at 47/83 Bd de l'Hôpital in Paris for use of the EM; Mireille Montcouquiol and Matthew Kelley for the anti-Vangl2 antibody and for making the *loop-tail* mice available; and Mathias Mericskay for technical expertise and helpful discussion. This work was supported by NIH-NCI RO1 9R01CA112686 to D.A.S. The Myology Group is the beneficiary of a strategic project plan support from the Association Française contre les Myopathies (AFM). Deposited in PMC for release after 12 months.

Supplementary material

Supplementary material for this article is available at http://dev.biologists.org/cgi/content/full/136/9/1559/DC1

References

Arango, N. A., Szotek, P. P., Manganaro, T. F., Oliva, E., Donahoe, P. K. and Teixeira, J. (2005). Conditional deletion of beta-catenin in the mesenchyme of the developing mouse uterus results in a switch to adipogenesis in the myometrium. *Dev. Biol.* **288**, 276-283.

Audebert, S., Navarro, C., Nourry, C., Chasserot-Golaz, S., Lecine, P., Bellaiche, Y., Dupont, J. L., Premont, R. T., Sempere, C., Strub, J. M. et al. (2004). Mammalian Scribble forms a tight complex with the betaPIX exchange factor. *Curr. Biol.* **14**, 987-995.

Bernard, P. and Harley, V. R. (2007). Wnt4 action in gonadal development and sex determination. *Int. J. Biochem. Cell Biol.* **39**, 31-43.

Bilder, D., Li, M. and Perrimon, N. (2000). Cooperative regulation of cell polarity and growth by Drosophila tumor suppressors. *Science* **289**, 113-116.

Bilder, D., Schober, M. and Perrimon, N. (2003). Integrated activity of PDZ protein complexes regulates epithelial polarity. *Nat. Cell Biol.* **5**, 53-58.

Boutin, E. L., Battle, E. and Cunha, G. R. (1992). The germ layer origin of mouse vaginal epithelium restricts its responsiveness to mesenchymal inductors: uterine induction. *Differentiation* **49**, 101-107.

Butz, S. and Larue, L. (1995). Expression of catenins during mouse embryonic development and in adult tissues. *Cell Adhes. Commun.* **3**, 337-352.

Carroll, E. A., Gerrelli, D., Gasca, S., Berg, E., Beier, D. R., Copp, A. J. and Klingensmith, J. (2003). Cordon-bleu is a conserved gene involved in neural tube formation. *Dev. Biol.* **262**, 16-31.

Carroll, T. J., Park, J. S., Hayashi, S., Majumdar, A. and McMahon, A. P. (2005). Wnt9b plays a central role in the regulation of mesenchymal to epithelial transitions underlying organogenesis of the mammalian urogenital system. *Dev. Cell* **9**, 283-292.

Carta, L. and Sassoon, D. (2004). Wnt7a is a suppressor of cell death in the female reproductive tract and is required for postnatal and estrogen-mediated growth. *Biol. Reprod.* **71**, 444-454.

Cunha, G. R. (1976a). Alterations in the developmental properties of stroma during the development of the urogenital ridge into ductus deferens and uterus in embryonic and neonatal mice. *J. Exp. Zool.* **197**, 375-388.

Cunha, G. R. (1976b). Epithelial-stromal interactions in development of the urogenital tract. *Int. Rev. Cytol.* **47**, 137-194.

Cunha, G. R. (1976c). Stromal induction and specification of morphogenesis and cytodifferentiation of the epithelia of the Mullerian ducts and urogenital sinus during development of the uterus and vagina in mice. *J. Exp. Zool.* **196**, 361-370.

Cunha, G. R., Battle, E., Young, P., Brody, J., Donjacour, A., Hayashi, N. and Kinbara, H. (1992a). Role of epithelial-mesenchymal interactions in the differentiation and spatial organization of visceral smooth muscle. *Epithelial Cell Biol.* **1**, 76-83.

Cunha, G. R., Young, P., Hamamoto, S., Guzman, R. and Nandi, S. (1992b). Developmental response of adult mammary epithelial cells to various fetal and neonatal mesenchymes. *Epithelial Cell Biol.* **1**, 105-118.

Cunha, G. R., Cooke, P. S. and Kurita, T. (2004). Role of stromal-epithelial interactions in hormonal responses. *Arch. Histol. Cytol.* **67**, 417-434.

Darken, R. S., Scola, A. M., Rakeman, A. S., Das, G., Mlodzik, M. and Wilson, P. A. (2002). The planar polarity gene strabismus regulates convergent extension movements in Xenopus. *EMBO J.* **21**, 976-985.

Deutscher, E. and Hung-Chang Yao, H. (2007). Essential roles of mesenchyme-derived beta-catenin in mouse Mullerian duct morphogenesis. *Dev. Biol.* **307**, 227-236.

Devenport, D. and Fuchs, E. (2008). Planar polarization in embryonic epidermis orchestrates global asymmetric morphogenesis of hair follicles. *Nat. Cell Biol.* **10**, 1257-1268.
Dow, L. E., Kauffman, J. S., Caddy, J., Zarbalis, K., Peterson, A. S., Jane, S. M., Russell, S. M. and Humbert, P. O. (2007). The tumour-suppressor Scribble dictates cell polarity during directed epithelial migration: regulation of Rho GTPase recruitment to the leading edge. *Oncogene* **26**, 2272-2282.
Glasser, S. R., Aplin, J. D., Giudice, L. C. and Tabibzadeh, S. (2002). *The Endometrium*. London: Informa Health Care.
Goto, T. and Keller, R. (2002). The planar cell polarity gene strabismus regulates convergence and extension and neural fold closure in Xenopus. *Dev. Biol.* **247**, 165-181.
Gumbiner, B. M. (1997). Carcinogenesis: a balance between beta-catenin and APC. *Curr. Biol.* **7**, R443-R446.
Guo, N., Hawkins, C. and Nathans, J. (2004). Frizzled6 controls hair patterning in mice. *Proc. Natl. Acad. Sci. USA* **101**, 9277-9281.
Hamblet, N. S., Lijam, N., Ruiz-Lozano, P., Wang, J., Yang, Y., Luo, Z., Mei, L., Chien, K. R., Sussman, D. J. and Wynshaw-Boris, A. (2002). Dishevelled 2 is essential for cardiac outflow tract development, somite segmentation and neural tube closure. *Development* **129**, 5827-5838.
Hardy, K. M., Garriock, R. J., Yatskievych, T. A., D'Agostino, S. L., Antin, P. B. and Krieg, P. A. (2008). Non-canonical Wnt signaling through Wnt5a/b and a novel Wnt11 gene, Wnt11b, regulates cell migration during avian gastrulation. *Dev. Biol.* **320**, 391-401.
Humbert, P., Russell, S. and Richardson, H. (2003). Dlg, Scribble and Lgl in cell polarity, cell proliferation and cancer. *BioEssays* **25**, 542-553.
Iguchi, T., Takase, M. and Takasugi, N. (1986). Development of vaginal adenosis-like lesions and uterine epithelial stratification in mice exposed perinatally to diethylstilbestrol. *Proc. Soc. Exp. Biol. Med.* **181**, 59-65.
Jessen, J. R., Topczewski, J., Bingham, S., Sepich, D. S., Marlow, F., Chandrasekhar, A. and Solnica-Krezel, L. (2002). Zebrafish trilobite identifies new roles for Strabismus in gastrulation and neuronal movements. *Nat. Cell Biol.* **4**, 610-615.
Kallay, L. M., McNickle, A., Brennwald, P. J., Hubbard, A. L. and Braiterman, L. T. (2006). Scribble associates with two polarity proteins, Lgl2 and Vangl2, via distinct molecular domains. *J. Cell. Biochem.* **99**, 647-664.
Kibar, Z., Vogan, K. J., Groulx, N., Justice, M. J., Underhill, D. A. and Gros, P. (2001). Ltap, a mammalian homolog of Drosophila Strabismus/Van Gogh, is altered in the mouse neural tube mutant Loop-tail. *Nat. Genet.* **28**, 251-255.
Kitajewski, J. and Sassoon, D. (2000). The emergence of molecular gynecology: homeobox and Wnt genes in the female reproductive tract. *BioEssays* **22**, 902-910.
Klein, T. J. and Mlodzik, M. (2005). Planar cell polarization: an emerging model points in the right direction. *Annu. Rev. Cell Dev. Biol.* **21**, 155-176.
Laura, R. P., Ross, S., Koeppen, H. and Lasky, L. A. (2002). MAGI-1: a widely expressed, alternatively spliced tight junction protein. *Exp. Cell Res.* **275**, 155-170.
Lechler, T. and Fuchs, E. (2005). Asymmetric cell divisions promote stratification and differentiation of mammalian skin. *Nature* **437**, 275-280.
Logan, C. Y. and Nusse, R. (2004). The Wnt signaling pathway in development and disease. *Annu. Rev. Cell Dev. Biol.* **20**, 781-810.
Lu, X., Borchers, A. G., Jolicoeur, C., Rayburn, H., Baker, J. C. and Tessier-Lavigne, M. (2004). PTK7/CCK-4 is a novel regulator of planar cell polarity in vertebrates. *Nature* **430**, 93-98.
Ludford-Menting, M. J., Oliaro, J., Sacirbegovic, F., Cheah, E. T., Pedersen, N., Thomas, S. J., Pasam, A., Iazzolino, R., Dow, L. E., Waterhouse, N. J. et al. (2005). A network of PDZ-containing proteins regulates T cell polarity and morphology during migration and immunological synapse formation. *Immunity* **22**, 737-748.
Ma, R. and Sassoon, D. A. (2006). PCBs exert an estrogenic effect through repression of the Wnt7a signaling pathway in the female reproductive tract. *Environ. Health Perspect.* **114**, 898-904.
Macara, I. G. (2004). Parsing the polarity code. *Nat. Rev. Mol. Cell Biol.* **5**, 220-231.
Mericskay, M., Kitajewski, J. and Sassoon, D. (2004). Wnt5a is required for proper epithelial-mesenchymal interactions in the uterus. *Development* **131**, 2061-2072.
Metais, J. Y., Navarro, C., Santoni, M. J., Audebert, S. and Borg, J. P. (2005). hScrib interacts with ZO-2 at the cell-cell junctions of epithelial cells. *FEBS Lett.* **579**, 3725-3730.
Miller, C. and Sassoon, D. A. (1998). Wnt-7a maintains appropriate uterine patterning during the development of the mouse female reproductive tract. *Development* **125**, 3201-3211.
Miller, C., Degenhardt, K. and Sassoon, D. A. (1998a). Fetal exposure to DES results in de-regulation of Wnt7a during uterine morphogenesis. *Nat. Genet.* **20**, 228-230.
Miller, C., Pavlova, A. and Sassoon, D. A. (1998b). Differential expression patterns of Wnt genes in the murine female reproductive tract during development and the estrous cycle. *Mech. Dev.* **76**, 91-99.
Mlodzik, M. (2002). Planar cell polarization: do the same mechanisms regulate Drosophila tissue polarity and vertebrate gastrulation? *Trends Genet.* **18**, 564-571.
Montcouquiol, M., Rachel, R. A., Lanford, P. J., Copeland, N. G., Jenkins, N. A. and Kelley, M. W. (2003). Identification of Vangl2 and Scrb1 as planar polarity genes in mammals. *Nature* **423**, 173-177.
Montcouquiol, M., Crenshaw, E. B., 3rd and Kelley, M. W. (2006a). Noncanonical Wnt signaling and neural polarity. *Annu. Rev. Neurosci.* **29**, 363-386.
Montcouquiol, M., Sans, N., Huss, D., Kach, J., Dickman, J. D., Forge, A., Rachel, R. A., Copeland, N. G., Jenkins, N. A., Bogani, D. et al. (2006b). Asymmetric localization of Vangl2 and Fz3 indicate novel mechanisms for planar cell polarity in mammals. *J. Neurosci.* **26**, 5265-5275.
Murdoch, J. N., Doudney, K., Paternotte, C., Copp, A. J. and Stanier, P. (2001). Severe neural tube defects in the loop-tail mouse result from mutation of Lpp1, a novel gene involved in floor plate specification. *Hum. Mol. Genet.* **10**, 2593-2601.
Murdoch, J. N., Henderson, D. J., Doudney, K., Gaston-Massuet, C., Phillips, H. M., Paternotte, C., Arkell, R., Stanier, P. and Copp, A. J. (2003). Disruption of scribble (Scrb1) causes severe neural tube defects in the circletail mouse. *Hum. Mol. Genet.* **12**, 87-98.
Nagasaka, K., Nakagawa, S., Yano, T., Takizawa, S., Matsumoto, Y., Tsuruga, T., Nakagawa, K., Minaguchi, T., Oda, K., Hiraike-Wada, O. et al. (2006). Human homolog of Drosophila tumor suppressor Scribble negatively regulates cell-cycle progression from G1 to S phase by localizing at the basolateral membrane in epithelial cells. *Cancer Sci.* **97**, 1217-1225.
Nakagawa, S., Yano, T., Nakagawa, K., Takizawa, S., Suzuki, Y., Yasugi, T., Huibregtse, J. M. and Taketani, Y. (2004). Analysis of the expression and localisation of a LAP protein, human scribble, in the normal and neoplastic epithelium of uterine cervix. *Br. J. Cancer* **90**, 194-199.
Navarro, C., Nola, S., Audebert, S., Santoni, M. J., Arsanto, J. P., Ginestier, C., Marchetto, S., Jacquemier, J., Isnardon, D., Le Bivic, A. et al. (2005). Junctional recruitment of mammalian Scribble relies on E-cadherin engagement. *Oncogene* **24**, 4330-4339.
Park, M. and Moon, R. T. (2002). The planar cell-polarity gene stbm regulates cell behaviour and cell fate in vertebrate embryos. *Nat. Cell Biol.* **4**, 20-25.
Parr, B. A. and McMahon, A. P. (1998). Sexually dimorphic development of the mammalian reproductive tract requires Wnt-7a. *Nature* **395**, 707-710.
Pavlova, A., Boutin, E., Cunha, G. and Sassoon, D. (1994). Msx1 (Hox-7.1) in the adult mouse uterus: cellular interactions underlying regulation of expression. *Development* **120**, 335-345.
Phillips, H. M., Murdoch, J. N., Chaudhry, B., Copp, A. J. and Henderson, D. J. (2005). Vangl2 acts via RhoA signaling to regulate polarized cell movements during development of the proximal outflow tract. *Circ. Res.* **96**, 292-299.
Phillips, H. M., Rhee, H. J., Murdoch, J. N., Hildreth, V., Peat, J. D., Anderson, R. H., Copp, A. J., Chaudhry, B. and Henderson, D. J. (2007). Disruption of planar cell polarity signaling results in congenital heart defects and cardiomyopathy attributable to early cardiomyocyte disorganization. *Circ. Res.* **101**, 137-145.
Phillips, H. M., Hildreth, V., Peat, J. D., Murdoch, J. N., Kobayashi, K., Chaudhry, B. and Henderson, D. J. (2008). Non-cell-autonomous roles for the planar cell polarity gene Vangl2 in development of the coronary circulation. *Circ. Res.* **102**, 615-623.
Qin, Y., Capaldo, C., Gumbiner, B. M. and Macara, I. G. (2005). The mammalian Scribble polarity protein regulates epithelial cell adhesion and migration through E-cadherin. *J. Cell Biol.* **171**, 1061-1071.
Rackow, B. W. and Arici, A. (2007). Reproductive performance of women with mullerian anomalies. *Curr. Opin. Obstet. Gynecol.* **19**, 229-237.
Shin, W. S., Maeng, Y. S., Jung, J. W., Min, J. K., Kwon, Y. G. and Lee, S. T. (2008). Soluble PTK7 inhibits tube formation, migration, and invasion of endothelial cells and angiogenesis. *Biochem. Biophys. Res. Commun.* **371**, 793-798.
Sinha, S. and Yang, W. (2008). Cellular signaling for activation of Rho GTPase Cdc42. *Cell Signal.* **20**, 1927-1934.
Strong, L. C. and Hollander, W. F. (1949). Hereditary loop-tail in the house mouse accompanied by inperforate vagina and with lethal craniorachischisis when homozygous. *J. Hered.* **40**, 329-334.
Tajbakhsh, S., Borello, U., Vivarelli, E., Kelly, R., Papkoff, J., Duprez, D., Buckingham, M. and Cossu, G. (1998). Differential activation of Myf5 and MyoD by different Wnts in explants of mouse paraxial mesoderm and the later activation of myogenesis in the absence of Myf5. *Development* **125**, 4155-4162.
Tanentzapf, G. and Tepass, U. (2003). Interactions between the crumbs, lethal giant larvae and bazooka pathways in epithelial polarization. *Nat. Cell Biol.* **5**, 46-52.
Torban, E., Wang, H. J., Groulx, N. and Gros, P. (2004). Independent mutations in mouse Vangl2 that cause neural tube defects in looptail mice impair interaction with members of the Dishevelled family. *J. Biol. Chem.* **279**, 52703-52713.

Wang, H. Y. and Malbon, C. C. (2003). Wnt signaling, Ca^{2+}, and cyclic GMP: visualizing Frizzled functions. *Science* **300**, 1529-1530.
Wang, J., Mark, S., Zhang, X., Qian, D., Yoo, S. J., Radde-Gallwitz, K., Zhang, Y., Lin, X., Collazo, A., Wynshaw-Boris, A. et al. (2005). Regulation of polarized extension and planar cell polarity in the cochlea by the vertebrate PCP pathway. *Nat. Genet.* **37**, 980-985.
Wang, J., Hamblet, N. S., Mark, S., Dickinson, M. E., Brinkman, B. C., Segil, N., Fraser, S. E., Chen, P., Wallingford, J. B. and Wynshaw-Boris, A. (2006a). Dishevelled genes mediate a conserved mammalian PCP pathway to regulate convergent extension during neurulation. *Development* **133**, 1767-1778.
Wang, Y., Guo, N. and Nathans, J. (2006b). The role of Frizzled3 and Frizzled6 in neural tube closure and in the planar polarity of inner-ear sensory hair cells. *J. Neurosci.* **26**, 2147-2156.
Wolff, T. and Rubin, G. M. (1998). Strabismus, a novel gene that regulates tissue polarity and cell fate decisions in Drosophila. *Development* **125**, 1149-1159.
Yao, R., Natsume, Y. and Noda, T. (2004). MAGI-3 is involved in the regulation of the JNK signaling pathway as a scaffold protein for frizzled and Ltap. *Oncogene* **23**, 6023-6030.
Yin, Y. and Ma, L. (2005). Development of the mammalian female reproductive tract. *J. Biochem.* **137**, 677-683.